

# A Single Mutation at the Ferredoxin Binding Site of P450 Vdh Enables Efficient Biocatalytic Production of 25-Hydroxyvitamin D<sub>3</sub>

Yoshiaki Yasutake,<sup>[a]</sup> Taiki Nishioka,<sup>[b, c]</sup> Noriko Imoto,<sup>[b, d]</sup> and Tomohiro Tamura<sup>\*[a, b]</sup>

Vitamin D<sub>3</sub> hydroxylase (Vdh) from *Pseudonocardia autotrophica* is a cytochrome P450 monooxygenase that catalyzes the two-step hydroxylation of vitamin D<sub>3</sub> (VD<sub>3</sub>) to produce 25-hydroxyvitamin D<sub>3</sub> (25(OH)VD<sub>3</sub>) and 1 $\alpha$ ,25-dihydroxyvitamin D<sub>3</sub> (1 $\alpha$ ,25(OH)<sub>2</sub>VD<sub>3</sub>). These hydroxylated forms of VD<sub>3</sub> are useful as pharmaceuticals for the treatment of conditions associated with VD<sub>3</sub> deficiency and VD<sub>3</sub> metabolic disorder. Herein, we describe the creation of a highly active T107A mutant of Vdh by engineering the putative ferredoxin-binding site. Crystallographic and kinetic analyses indicate that the T107A mutation results in conformational change from an open to a closed

state, thereby increasing the binding affinity with ferredoxin. We also report the efficient biocatalytic synthesis of 25(OH)VD<sub>3</sub>, a promising intermediate for the synthesis of various hydroxylated VD<sub>3</sub> derivatives, by using nisin-treated *Rhodococcus erythropolis* cells containing Vdh<sub>T107A</sub>. The gene-expression cassette encoding *Bacillus megaterium* glucose dehydrogenase-IV was inserted into the *R. erythropolis* chromosome and expressed to avoid exhaustion of NADH in a cytoplasm during bioconversion. As a result, approximately 573  $\mu\text{g mL}^{-1}$  25(OH)VD<sub>3</sub> was successfully produced by a 2 h bioconversion.

## Introduction

Microbial processing is more efficient and friendly to the environment than chemical synthesis, because of its specificity and minimal use of organic solvents. Cytochrome P450 monooxygenases (P450s) are of special interest for the production of fine chemicals and pharmaceuticals because of their ability to insert oxygen into the nonactivated C–H bonds of various compounds, in a regio- and stereoselective manner and under mild conditions.<sup>[1]</sup> Generally, selective C–H bond oxygenation is one of the most challenging processes in synthetic chemistry; therefore, P450s are attractive candidates as biocatalysts in biotechnological applications.<sup>[2]</sup> P450s are heme-containing enzymes that use molecular oxygen and two-electron transfer from a hydride donor NAD(P)H via appropriate redox partner proteins (e.g., ferredoxin (Fdx) and ferredoxin reductase (FdxR))

for catalytic reactions.<sup>[3]</sup> They are involved in many physiological roles, including the biosynthesis of steroids, fatty acids, and complex antibiotics, and biological processes such as lipid homeostasis, detoxifying xenobiotics, and drug metabolism.<sup>[4–7]</sup>

Vitamin D<sub>3</sub> (VD<sub>3</sub>) is a secosteroid, which is similar in structure to a steroid but has an opened B-ring. In humans, VD<sub>3</sub> is obtained from the diet or is synthesized from 7-dehydrocholesterol within the skin in response to sunlight. VD<sub>3</sub> is further converted into the active forms of VD<sub>3</sub>, 25-hydroxyvitamin D<sub>3</sub> (25(OH)VD<sub>3</sub>), in the liver, and then to 1 $\alpha$ ,25-dihydroxyvitamin D<sub>3</sub> (1 $\alpha$ ,25(OH)<sub>2</sub>VD<sub>3</sub>) in the kidney. Both steps are catalyzed by several P450s.<sup>[8–11]</sup> The active forms of VD<sub>3</sub> regulate calcium homeostasis through interactions with VD<sub>3</sub> receptors in major tissues, bone, and the intestine. Thus, VD<sub>3</sub> metabolic disorders lead to low serum calcium levels (hypocalcemia) and defective mineralization of the bone matrix. Moreover, active forms of VD<sub>3</sub> function as hormones and play critical roles in controlling differentiation and proliferation of multiple cell types. Hydroxylated VD<sub>3</sub> and its derivatives are currently used as pharmaceuticals for the treating the symptoms of numerous disorders, such as rickets, osteomalacia, osteoporosis, hypoparathyroidism, and psoriasis.<sup>[12]</sup> Although chemical synthesis of 1 $\alpha$ ,25(OH)<sub>2</sub>VD<sub>3</sub> from cholesterol is an established method, it is inefficient (yield  $\leq 1\%$ ).<sup>[13]</sup> In contrast, microbial conversion using actinomycete *Pseudonocardia autotrophica* cells is practical for the production of 25(OH)VD<sub>3</sub> and 1 $\alpha$ ,25(OH)<sub>2</sub>VD<sub>3</sub>.<sup>[14, 15]</sup> *P. autotrophica* possesses P450 Vdh (CYP107BR1), a cytochrome P450 monooxygenase that hydroxylates VD<sub>3</sub>. However, this microbial conversion requires a long reaction time (72 h for the production of 137  $\mu\text{g mL}^{-1}$  25(OH)VD<sub>3</sub> under optimized culture conditions).<sup>[15]</sup>


[a] Dr. Y. Yasutake,<sup>\*</sup> Prof. T. Tamura  
Bioproduction Research Institute  
National Institute of Advanced Industrial Science and Technology (AIST)  
2-17-2-1, Tsukisamu-higashi, Toyohira-ku, Sapporo 062-8517 (Japan)  
E-mail: t-tamura@aist.go.jp

[b] Dr. T. Nishioka,<sup>\*</sup> Dr. N. Imoto, Prof. T. Tamura  
Graduate School of Agriculture, Hokkaido University  
Kita-9, Nishi-9, Kita-ku, Sapporo 060-8589 (Japan)

[c] Dr. T. Nishioka<sup>\*</sup>  
Current address: MicroBiopharm Japan, Co. Ltd.  
1808 Nakaizumi, Iwata, Shizuoka 438-0078 (Japan)

[d] Dr. N. Imoto  
Current address:  
Department of Human Health Science, Hachinohe Gakuin University  
13–98 Mihono, Hachinohe, Aomori 031-8588 (Japan)

[\*] These authors contributed equally to this work.

 Supporting information for this article is available on the WWW under <http://dx.doi.org/10.1002/cbic.201300386>.

To develop a more efficient method for the hydroxylation of  $\text{VD}_3$ , we have used a recombinant system by using *Rhodococcus erythropolis* cells.<sup>[16]</sup> There are three problems to overcome: permeability of  $\text{VD}_3$  across the cell membrane is limited;<sup>[17]</sup> the catalytic activity of Vdh is relatively low because  $\text{VD}_3$  is probably a nonnative substrate for Vdh; and, sufficient electrons are needed for the catalytic turnover of P450. To address the first issue (permeability), we recently developed a technique in which pore structures in the *Rhodococcus* cell membrane are generated by a small antimicrobial peptide (nisin) to improve the permeability of  $\text{VD}_3$  into the cytoplasm.<sup>[18]</sup> For the second issue (catalytic activity), we constructed a quadruple mutant of Vdh (Vdh-K1: T70R/V156L/E216M/E384R) by directed evolution.<sup>[16]</sup> Unfortunately, the expression level of Vdh-K1 was very low in *R. erythropolis* cells, and, thus, was not suitable for *R. erythropolis* bioconversion. To date, several research groups have attempted to increase the productivity of active forms of  $\text{VD}_3$ . Fujii et al. reported 2.2-fold more efficient  $\text{VD}_3$  bioconversion with *Escherichia coli*, by disruption of efflux pump genes (*AcrAB/TolC*).<sup>[19]</sup> Hayashi and co-workers reported bioconversion from  $\text{VD}_3$  to several species of hydroxylated  $\text{VD}_3$  metabolites by using a *Streptomyces* strain expressing CYP105A1.<sup>[20–22]</sup> Nevertheless, a dramatic improvement in the production of hydroxylated  $\text{VD}_3$  has not been realized.

Herein, we report the creation of a highly active single mutant of Vdh (Vdh<sub>T107A</sub>) by engineering the putative Fdx-binding site. Vdh<sub>T107A</sub> was well expressed as an active heme-containing form in *R. erythropolis* cells. In addition, the gene encoding *Bacillus megaterium* glucose dehydrogenase was inserted into the chromosome of *R. erythropolis* JCM3201 and was expressed to provide a stable supply of NADH. Electrons were thus donated to Vdh from NADH by coexpressing the redox partner proteins, AcIB (Fdx) and AcIC (FdxR). Partially methylated  $\beta$ -cyclodextrin (PM $\beta$ CD) was used to reduce 25(OH) $\text{VD}_3$  1 $\alpha$ -hydroxylation activity,<sup>[15]</sup> as well as to increase the water solubility of  $\text{VD}_3$ . As a result, an exceptionally high yield of 25(OH) $\text{VD}_3$  (a promising intermediate for the synthesis of various hydroxylated  $\text{VD}_3$  derivatives)<sup>[23]</sup> was achieved by using nisin-treated *R. erythropolis* cells.

## Results and Discussion

### Selection of redox partner proteins coupled with Vdh

Most bacterial P450s require two electrons sequentially delivered from NAD(P)H via redox partner proteins (e.g., FAD-containing FdxR, and the small iron–sulfur protein Fdx). Unfortunately, the native redox partner proteins for Vdh in *P. autotrophica* cells remain unknown. To select appropriate redox partner proteins for  $\text{VD}_3$  bioconversion by *R. erythropolis* cells, we tested seven pairs of recombinant Fdx/FdxR proteins from *R. erythropolis* JCM3201. However, no useful redox partners were found. Therefore, we used AcIB (Fdx) and AcIC (FdxR) proteins from *Acinetobacter* sp. OC4<sup>[24]</sup> as redox partner proteins for Vdh. We have previously reported that AcIB/AcIC can reasonably be coupled with Vdh, both in vivo and in vitro.<sup>[18]</sup>

### Site-directed mutagenesis at the Fdx binding site of Vdh

Generally, the combination of native P450 and Fdx showed a high electron-transfer rate from Fdx to P450 and, consequently, catalytic efficiency.<sup>[25]</sup> If the native redox partner for a particular P450 is unknown, site-directed mutagenesis of the putative Fdx/P450 association site is an attractive strategy for increasing P450s catalytic activity.<sup>[26–28]</sup> Therefore, in order to improve the  $\text{VD}_3$  hydroxylating activity of Vdh, the amino-acid residues at putative Fdx-binding sites of Vdh were substituted with those from P450 AcIA (CYP153A), an enzyme naturally coupled with AcIB in *Acinetobacter* sp. OC4.<sup>[24]</sup> As the X-ray structure of P450 AcIA has not been reported, the amino-acid residues involved in Fdx binding were identified based on the X-ray structure of P450cam from *Pseudomonas putida* (PDB ID: 2CPP; the best-characterized P450, including the intermolecular interactions with putidaredoxin (Fdx) by X-ray and NMR analyses,<sup>[29–33]</sup> site-directed mutagenesis,<sup>[34]</sup> and molecular docking simulations).<sup>[35,36]</sup> In total, eight residues were selected for mutational analysis; the corresponding residues of AcIA were identified by sequence alignment in CLUSTALW<sup>[37]</sup> (Figures S1 and S2 in the Supporting Information). The mutants created and the  $\text{VD}_3$  25-hydroxylase activities for these mutants are summarized in Table 1.  $\text{VD}_3$  25-hydroxylase activity

**Table 1.** Comparison of specific activities of Vdh<sub>WT</sub> and mutants against  $\text{VD}_3$ .

Variant	$\text{VD}_3$ 25-hydroxylase activity [mol min <sup>−1</sup> per mol of P450]	Relative activity
Vdh <sub>WT</sub>	0.07 ± 0.01	1.0
Vdh-K1 (T70R/V156L/E216M/E384R)	5.42 ± 0.45	77.4
T96D	0.03 ± 0.01	0.5
F106V	n.d.	
T107A	5.54 ± 0.56	79.2
V108P	0.05 ± 0.00	0.7
F346R	0.08 ± 0.01	1.2
Q351R	0.15 ± 0.02	2.2
H342F	0.10 ± 0.01	1.4
L348M	n.d.	
n.d.: not detected.		

with mutations T107A, H342F, F346R, or Q351R was elevated compared to wild-type (Vdh<sub>WT</sub>); two mutants (F106V and L348M) showed no catalytic activity. Interestingly, Vdh<sub>T107A</sub> exhibited exceptionally high  $\text{VD}_3$  25-hydroxylating activity (~80 times higher than Vdh<sub>WT</sub>). This activity level is comparable to that of Vdh-K1, a quadruple Vdh mutant generated by directed evolution.<sup>[16]</sup>

### Kinetic analysis

To evaluate kinetic parameters describing the enzymatic changes, we performed a reconstituted in vitro enzyme assay, and measured  $\text{VD}_3$  25-hydroxylase activity with varying concentration of AcIB;  $K_m$  and  $k_{cat}$  were calculated by fitting Mi-

**Table 2.** Kinetic parameters for AcIB on VD<sub>3</sub> 25-hydroxylation activity.

	$K_m$ [ $\mu\text{M}$ ]	$k_{\text{cat}}$ [ $\text{min}^{-1}$ ]	$k_{\text{cat}}/K_m$ [ $\text{min}^{-1} \text{M}^{-1}$ ]
Vdh <sub>WT</sub>	$85.7 \pm 8.4$	$0.81 \pm 0.18$	$9.45 \times 10^3$
Vdh <sub>T107A</sub>	$24.5 \pm 3.8$	$23.0 \pm 1.40$	$9.39 \times 10^5$
Vdh-K1	$19.7 \pm 4.1$	$20.8 \pm 1.37$	$1.06 \times 10^6$

chaelis–Menten plots for Vdh<sub>WT</sub>, Vdh-K1, and Vdh<sub>T107A</sub> (Table 2). The results show that  $k_{\text{cat}}$  increased from 0.81 to 23.0  $\text{min}^{-1}$ , and  $K_m$  decreased from 85.7 to 24.5  $\mu\text{M}$ , for the single mutation T107A. Interestingly, Vdh-K1 exhibited similar kinetic properties to Vdh<sub>T107A</sub>. These results indicate that the four mutations of Vdh-K1 and the single mutation of Vdh<sub>T107A</sub> lead to similar changes in the enzymatic properties related to the enhancement of the binding affinity to AcIB (Table 2).

VD<sub>3</sub> 25-hydroxylation activity was also measured with commercially available spinach Fdx/FdxR, which is commonly used as a redox partner protein pair for in vitro reconstituted P450 assays. The results showed that the VD<sub>3</sub> 25-hydroxylation activity of both Vdh-K1 and Vdh<sub>T107A</sub> increased ~50-fold (Table S1), similar to the results obtained with AcIB/AicC. This suggests that the T107A mutation and the four mutations of Vdh-K1 do not contribute to improvement in AcIB specificity, but affect the underlying catalytic mechanism of Vdh and thus bring about high catalytic efficiency. A single mutation at the molecular surface might seem trivial; however, the T107A mutation confers upon Vdh the ability to function at a level approximate equivalent to that of Vdh-K1. Our previous structural and spectroscopic studies indicated that the conformational change from an open to a closed state (resulting from the four mutations in Vdh-K1) led to a dramatic increase in catalytic activity.<sup>[38]</sup> Therefore, it would be of great interest to determine the structure of Vdh<sub>T107A</sub>. Investigations should determine whether it is possible to change the conformation of Vdh by just removing the hydroxyl and methyl groups of Thr107.

### Crystal structure of Vdh<sub>T107A</sub> exhibits a closed conformation

Crystals of Vdh<sub>T107A</sub> with different morphology can be obtained from different crystallization solutions, and compared to those of Vdh<sub>WT</sub> and Vdh-K1. The crystallization conditions used for Vdh<sub>WT</sub> and Vdh-K1 did not yield crystals of Vdh<sub>T107A</sub>. The structure of Vdh<sub>T107A</sub> in a complex with VD<sub>3</sub> was solved at a resolution of 2.57 Å by molecular replacement. The asymmetric unit comprises a single monomer (Matthews coefficient,  $V_m = 2.53 \text{ Å}^3 \text{Da}^{-1}$ ). The final refined model consists of amino acid residues 2 to 403, the heme cofactor, VD<sub>3</sub>, and 36 water molecules, with crystallographic  $R$  and  $R_{\text{free}}$  factors of 0.187 and 0.231, respectively (crystallographic parameters and refinement statistics are summarized in Table 3). The electron density was of high quality, thus allowing good definition of the model, with the exception of the C-terminal His tag region.

The structure of Vdh<sub>T107A</sub> was superimposed onto that of Vdh-K1 (which forms a closed conformation) with a root mean square deviation (RMSD) of 0.7 Å for 390 C $\alpha$  atoms (Figures 1 and S3, and Movie S1). The results clearly show that Vdh<sub>T107A</sub>

**Table 3.** Crystallographic parameters and model refinement statistics of Vdh<sub>T107A</sub>.

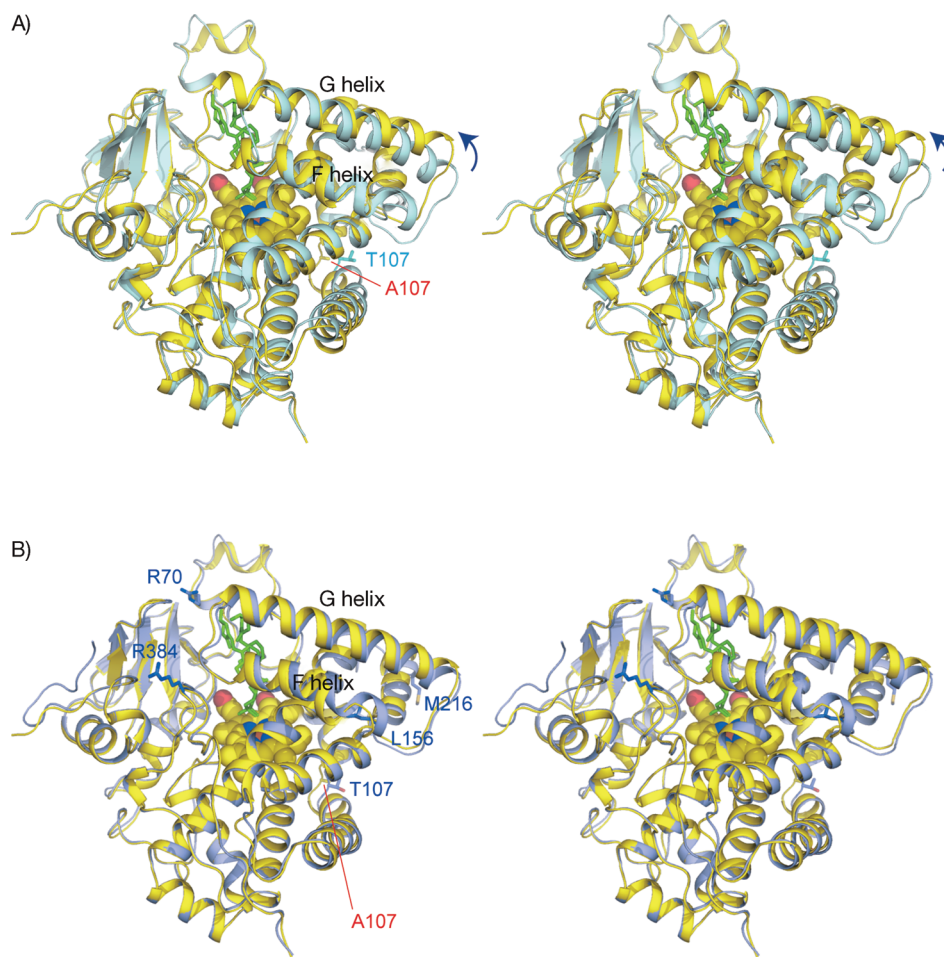
Data collection statistics	
beamline	BL-5A, PF
wavelength [Å]	1.0000
resolution [Å]	50–2.57 (2.64–2.57) <sup>[a]</sup>
unit cell dimensions	
$a$ , $b$ , $c$ [Å]	61.4, 105.5, 142.0
space group	C222 <sub>1</sub>
unique reflections	14 156
$R_{\text{sym}}$ <sup>[b]</sup>	0.048 (0.557) <sup>[a]</sup>
completeness [%]	98.6 (92.3) <sup>[a]</sup>
redundancy	5.8 (5.6)
mean $I/\sigma(I)$	24.2 (3.1) <sup>[a]</sup>
Refinement statistics and model quality	
resolution range [Å]	50–2.57
$R_{\text{work}}$ <sup>[c]</sup>	0.187
$R_{\text{free}}$ <sup>[d]</sup>	0.231
total number of atoms	3212
average $B$ factor [Å <sup>2</sup> ]	76.7
RMSD bond distances [Å]	0.008
RMSD bond angles [°]	1.93

[a] Values in parentheses refer to data in the highest resolution shell. [b]  $R_{\text{sym}} = \sum_i \sum_j |I_{ij} - \langle I_i \rangle| / \sum_i \sum_j I_{ij}$ , where  $\langle I_i \rangle$  is the mean intensity of a set of equivalent reflections. [c]  $R_{\text{work}} = \sum |F_{\text{obs}} - F_{\text{calc}}| / \sum F_{\text{obs}}$  for 95 % of the reflection data used in the refinement.  $F_{\text{obs}}$  and  $F_{\text{calc}}$  are the observed and calculated structure factor amplitudes, respectively. [d]  $R_{\text{free}}$  is the equivalent of  $R_{\text{work}}$  except that it was calculated for a randomly chosen 5 % test set excluded from refinement.

exhibits a closed conformation similar to that of Vdh-K1 bound to VD<sub>3</sub>. Main-chain and side-chain conformations at the active-site region of Vdh<sub>T107A</sub> superimposed well onto those of Vdh-K1 (Figure S5). The closed conformation of Vdh can be characterized by the ~8 Å shift of the helices F/G and the local conformational change around the HI-loop (nomenclature of the secondary structure elements follows the established convention).<sup>[38]</sup> In the structure of Vdh<sub>T107A</sub>, Asp219 in the HI-loop contacts neighboring monomers in the crystal lattice; no crystal contacts were found in the vicinity of helices F/G, which directly cover the substrate-binding site and separate it from the solvent. Therefore, we assume that the current closed form of Vdh<sub>T107A</sub> is not a crystallization artifact but reflects the conformational state in solution. P450 is generally considered exhibit conformational dynamics (between open and closed states) in solution,<sup>[39–42]</sup> and, thus, similarly to Vdh-K1, the T107A mutation might be responsible for the shift in the conformational equilibrium towards the closed state. Molecular dynamic simulation is currently underway to demonstrate how the mutation affects the conformational dynamics of Vdh.

It is known that, in general, the P450-binding surface of Fdx is negatively charged and the Fdx-binding surface of P450 is positively charged. These opposite electrostatic characteristics of the molecular surfaces are known to be responsible for the association between P450 and Fdx.<sup>[35,43,44]</sup> Kinetic studies have shown that the AcIB-binding affinities of Vdh-K1 and Vdh<sub>T107A</sub> were approximately threefold higher than that of Vdh<sub>WT</sub>. We therefore calculated the electrostatic charge distributions for Vdh<sub>WT</sub>, Vdh-K1, and Vdh<sub>T107A</sub>. Evidently, the electrostatic charge potentials of the Fdx-binding surfaces of Vdh<sub>T107A</sub> and Vdh-K1





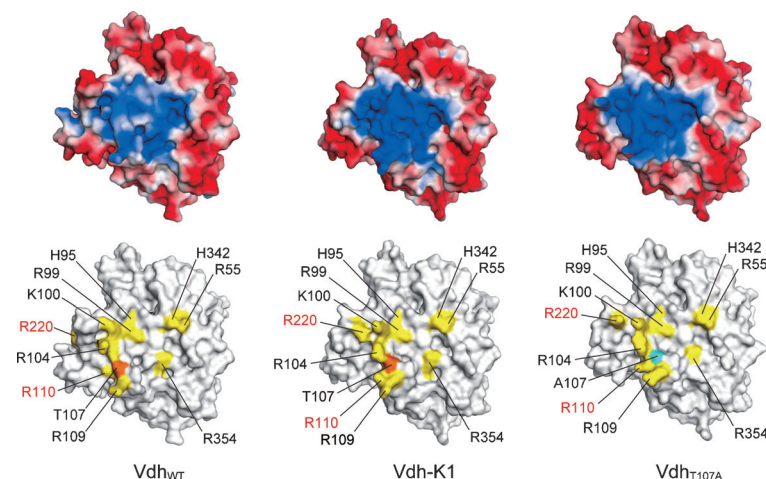
**Figure 1.** Stereoview superimpositions of X-ray structures of A)  $Vdh_{WT}$  (cyan, open conformation) and  $Vdh_{T107A}$  (yellow, closed conformation), and B)  $Vdh$ -K1 (purple, closed conformation) and  $Vdh_{T107A}$  (yellow, closed conformation). Side chains of the mutated residues in  $Vdh_{T107A}/Vdh$ -K1 are shown as sticks and labeled; mobile F- and G-helices are labeled; bound  $VD_3$  is shown as sticks (green).

exhibit a more positively charged potential than that of  $Vdh_{WT}$ , thus indicating that the closed conformation could be more suitable for Fdx association (Figure 2). Although there are no remarkable changes in the overall structure of helices and loops of the Fdx-binding surface, subtle conformational changes in the CD helices are evident. In addition, there are significant alterations to the side-chain conformations of Arg110 (D-helix) and Arg220 (HI-loop; Figure 2). It is likely that these changes affect the electrostatic charge distribution on the Fdx-binding surface. We also found similar difference in electrostatic surface potential in P450 PikC (CYP107L1; PDB ID: 2BVJ), the P450 structure most homologous to Vdh.<sup>[39]</sup> Structures of substrate-free PikC have been solved in both open and closed conformations. Similarly to Vdh, the Fdx-binding surface of the closed form of PikC is more positively charged than that in open form (Figure S6). These observations indicate that the conformational change from an open to a closed state could be important for association with Fdx and sub-

strate binding. Searching for mutation loci affecting conformational equilibrium is an interesting approach to identify useful mutants of a target P450 enzyme for improved activity.

### Bioconversion of $VD_3$ to $25(OH)VD_3$ in nisin-treated *R. erythropolis* cells

Recently, we have developed a biocatalytic conversion system that uses nisin-treated *R. erythropolis* cells.<sup>[18]</sup> Nisin is a natural antimicrobial polypeptide and plays a role in increasing  $VD_3$  permeability across the cell membrane (by forming a pore in the cell membrane). Previous studies demonstrated that nisin inhibits cell growth of actinomycetes by forming pores, thus leading to efflux of many vital intracellular compounds. However, proteins with relatively large molecular weight do not leak out, as the diameter of the nisin-forming pore is no more than 2.0–2.5 nm.<sup>[45,46]</sup> Importantly, nisin does not cause lysis of *R. erythropolis* cells, and, thus, nisin-treated dead *R. erythropolis* cells are useful as a biocatalytic system: overexpressed enzymes



**Figure 2.** Electrostatic potentials of Fdx-binding surfaces of  $Vdh_{WT}$ ,  $Vdh$ -K1, and  $Vdh_{T107A}$ . Potentials were calculated with the Adaptive Poisson–Boltzmann solver (APBS), and are presented in the range  $-4$  (red) to  $+44$  kT/e (blue). The same surface models showing the positions of basic residues and the mutated residue T107/A107 on the Fdx-binding surface are shown below. Arg220 and Arg110, which probably contribute to the change in electrostatic potential, are indicated in red (see text).

for the bioconversion reaction are retained in the cytoplasm. In our previous study,  $\text{VD}_3$  bioconversion to  $25(\text{OH})\text{VD}_3$  was performed by using nisin-treated *R. erythropolis* JCM3201 cells that coexpressed  $\text{Vdh}_{\text{WT}}$  and redox partner proteins  $\text{AciB}$  and  $\text{AciC}$ .<sup>[18]</sup>  $\text{NADH}$  and *B. megaterium* glucose dehydrogenase IV ( $\text{BmGlcDH-IV}$ )<sup>[47,48]</sup> were added to the bioconversion solution to maintain a supply of  $\text{NADH}$  to  $\text{P450}$ . However, the  $\text{Vdh-K1}$  mutant obtained by directed evolution could not be well expressed in *R. erythropolis* cells; thus, its performance was not suitable for this system. Indeed, the thermostability of  $\text{Vdh-K1}$  was found to be lower than that of  $\text{Vdh}_{\text{WT}}$  and  $\text{Vdh}_{\text{T107A}}$  (Figure S7).

The activity of  $\text{Vdh}_{\text{T107A}}$  is comparable to that of  $\text{Vdh-K1}$ . The thermostability of  $\text{Vdh}_{\text{T107A}}$  is comparable to that of  $\text{Vdh}_{\text{WT}}$  (Figure S7), and  $\text{Vdh}_{\text{T107A}}$  can be reliably overexpressed in *R. erythropolis* cells: the expression level of  $\text{Vdh}_{\text{T107A}}$  is approximately 70% of that of  $\text{Vdh}_{\text{WT}}$ . Prior to the bioconversion test, we adapted *R. erythropolis* JCM3201 to incorporate the  $\text{BmGlcDH-IV}$  gene in its chromosome by a random transposon mutagenic system,<sup>[49]</sup> to maintain a supply of  $\text{NADH}$  within the cytoplasm. The resulting strain was termed JCM3201-GlcDH. A schematic diagram of the bioconversion is shown in Figure 3, and the results of the bioconversion are given in Figure 4. Bioconversion with nisin-treated *R. erythropolis* JCM3201-GlcDH containing  $\text{Vdh}_{\text{T107A}}$  was the most effective: almost  $300 \mu\text{g mL}^{-1}$  of  $25(\text{OH})\text{VD}_3$  was produced after only 2 h of bioconversion (Figure 4A). We then performed repeated production of  $25(\text{OH})\text{VD}_3$ , based on previously described procedures.<sup>[18]</sup> The reaction solution (5 mL) was refreshed every 2 h, and four consecutive conversion reactions (total ca. 8 h) were carried out under optimized conditions (0.2 mM  $\text{NADH}$ ,  $\text{OD}_{600} = 10.0$ ). It is likely that iterative bioconversion reactions result in degradation or loss of biocatalyst (nisin-treated cells containing  $\text{Vdh}_{\text{T107A}}$  and other proteins) by harvesting and resuspension. However, the activity level was still approximately 60% after three cycles (Figure 4B), and the total amount of  $25(\text{OH})\text{VD}_3$  obtained by this biocatalyst-reusing method was approximate-

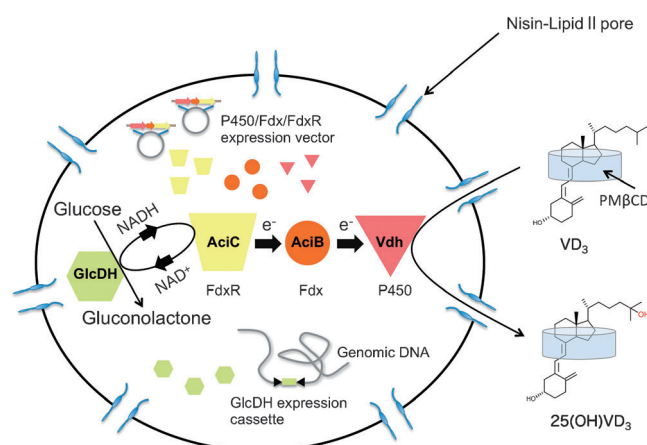


**Figure 3.** Nisin-treated *R. erythropolis* JCM3201-GlcDH bioconversion of  $\text{VD}_3$  into  $25(\text{OH})\text{VD}_3$ .  $\text{PMBCD}$  was used to increase the solubility of  $\text{VD}_3$ / $25(\text{OH})\text{VD}_3$ , as well as to reduce second-step hydroxylation (see text). The pore in the cell membrane generated by nisin treatment afforded permeability of the  $\text{PMBCD-VD}_3$  complex.

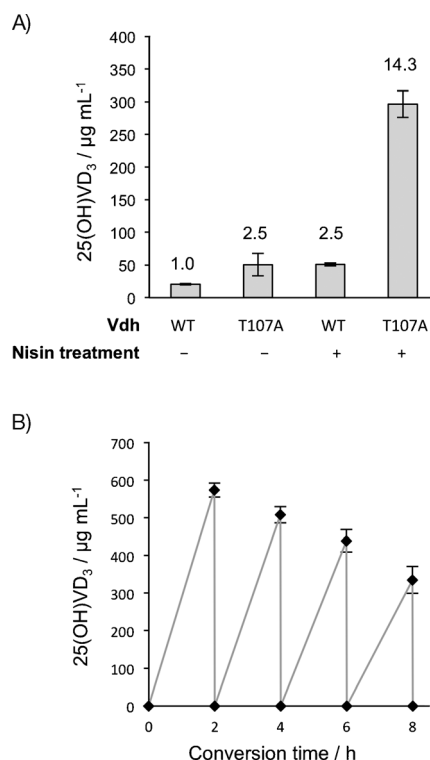


**Figure 4.** Biocatalytic production of  $25(\text{OH})\text{VD}_3$  by nisin-treated *R. erythropolis* JCM3201-GlcDH cells containing  $\text{Vdh}_{\text{T107A}}$ . A) Effect of T107A mutation on bioconversion; the relative amounts of  $25(\text{OH})\text{VD}_3$  production are shown. The combination of nisin treatment and  $\text{Vdh}_{\text{T107A}}$  resulted in an approximately 14-fold increase in bioconversion efficiency. B) Repeated biocatalytic production of  $25(\text{OH})\text{VD}_3$  according to the same procedure but with reaction-buffer refreshment every 2 h. In this experiment, double the amount of cells was used compared to (A); see the Experimental Section. Error bars indicate standard deviation of three independent experiments.

**Table 4.** Bioconversion of  $\text{VD}_3$  into  $25(\text{OH})\text{VD}_3$  in this and previous studies.

Species	Enzyme	25(OH)VD <sub>3</sub> production [μg mL <sup>-1</sup> ]	Reaction time [h]	Ref.
<i>P. autotrophica</i>	$\text{Vdh}_{\text{WT}}$	137	48	[15]
<i>E. coli</i>	$\text{Vdh}_{\text{WT}}$	216	24	[19]
<i>Streptomyces lividans</i>	CYP105A1 (R73V/R84A)	7.8	24	[20]
<i>R. erythropolis</i>	$\text{Vdh}_{\text{WT}}$	342	16 <sup>[a]</sup>	[18]
<i>R. erythropolis</i>	$\text{Vdh}_{\text{T107A}}$	573	2	this study

[a] This value (not given in the literature) was calculated from the raw data.

ly 9 mg. Production of  $25(\text{OH})\text{VD}_3$  in this and previously studies is summarized in Table 4.

## Conclusions

We obtained a highly active  $\text{Vdh}$  mutant ( $\text{Vdh}_{\text{T107A}}$ ) by engineering the putative  $\text{Fdx}$ -binding site. In vitro reconstituted assay showed that  $\text{Vdh}_{\text{T107A}}$  was approximately 80 times more active than  $\text{Vdh}_{\text{WT}}$ . Kinetic analyses indicate that  $\text{Vdh}_{\text{T107A}}$  has

improved binding affinity with *Acinetobacter* Fdx (AcIB), thereby improving  $\text{VD}_3$  hydroxylation activity. The crystal structure of  $\text{Vdh}_{\text{T107A}}$  exhibited a closed conformation similar to that of  $\text{Vdh-K1}$ , a highly active quadruple mutant acquired by directed evolution. Similarly to  $\text{Vdh-K1}$ , it is likely that the T107A mutation is responsible for the shift in the conformational equilibrium in solution from the open to the closed state. The electrostatic surface distribution revealed that the Fdx-binding site of the closed conformation was more positively charged than that of the open conformation. These observations suggest that the closed form is more suitable for binding to negatively charged Fdx. Finally, we tested  $\text{VD}_3$  bioconversion to  $25(\text{OH})\text{VD}_3$  by using nisin-treated *R. erythropolis* JCM3201-GlcDH (coexpressed  $\text{Vdh}_{\text{T107A}}$ /AcIB/AciC), and showed exceptionally high yield of  $25(\text{OH})\text{VD}_3$ .  $\text{VD}_3$  bioconversion by nisin-treated *R. erythropolis* JCM3201-GlcDH represents a simple strategy and application, and could be widely useful for P450-mediated conversion of other fat-soluble and/or toxic molecules for living cells coexpressing appropriate redox partner proteins.

## Experimental Section

**Materials:** *R. erythropolis* JCM3201 (Japan Collection of Microorganisms), *E. coli* XL1-Blue, and *E. coli* BL21-CodonPlus(DE3)-RIL cells were routinely cultured in lysogeny broth (LB). Competent cells of *R. erythropolis* were prepared according to the procedure outlined by Shao et al.<sup>[50]</sup> Transformation of *R. erythropolis* JCM3201 was performed according to a previously described method.<sup>[51]</sup> Oligonucleotides were obtained from Hokkaido System Science (Sapporo, Japan). PCR was performed with *Pfu* Turbo DNA polymerase (Stratagene/Agilent) or KOD FX polymerase (Toyobo, Osaka, Japan). Restriction endonucleases were purchased from New England Biolabs and Promega. The DNA ligation kit was purchased from Takara Bio (Shiga, Japan). A Wizard SV Gel and PCR Clean-Up System (Promega) was used to purify PCR products from gel before cloning or sequencing. DNA was sequenced with a BigDye Terminator v3.1 Cycle Sequencing Kit (Applied Biosystems/Life Technologies) on an ABI Prism 3100 automated sequencer (Applied Biosystems) according to the manufacturer's instructions.

**Overexpression and purification of recombinant protein for in vitro assay:** Recombinant and mutant  $\text{Vdh}$  for the in vitro assay contained a C-terminal His<sub>6</sub> tag.  $\text{Vdh}$  mutants were prepared by inverse PCR<sup>[52]</sup> with synthetic oligonucleotide primers and pET29b- $\text{Vdh}_{\text{WT}}$ <sup>[38]</sup> as the template. Recombinant  $\text{Vdh}_{\text{WT}}$  and mutants were produced in *E. coli* BL21 CodonPlus (DE3)-RIL, and purified as previously described.<sup>[38]</sup> A carbon monoxide difference spectra assay was performed to assess  $\text{Vdh}$  concentration.<sup>[53]</sup>

The gene encoding AcIB from *Acinetobacter* sp. OC4 (Gene Bank accession: AB221118) was amplified by PCR with pTipQC2- $\text{Vdh}$ -AcIB-AciC as template DNA,<sup>[18]</sup> and inserted between the NdeI and XhoI sites of the pET28a expression vector. Transformed *E. coli* cells were grown at 37 °C in LB medium (100 mL), then overnight culture was inoculated into LB (900 mL). Expression was induced by addition of isopropyl- $\beta$ -D-thiogalactoside (IPTG, 0.1 mM), and the cells were cultured overnight at 25 °C. Cells were harvested by centrifugation (2975 g, 10 min, 4 °C) and resuspended in buffer A (Tris-HCl (50 mM, pH 7.5), NaCl (100 mM), glycerol (10%)) containing lysozyme (1 mg mL<sup>-1</sup>) and Benzonase (50 U mL<sup>-1</sup>; Merck Millipore). The cells were disrupted by sonication, and the homogenate was clarified by centrifugation (39 191 g, 10 min, 4 °C). The superna-

tant was loaded onto a Ni-affinity column (Sigma-Aldrich) equilibrated with buffer A, and then eluted with a linear gradient of imidazole (0–0.4 M in buffer A). The brown-colored fractions were pooled, and the concentrated sample was further purified on a Sephacryl S-100 size-exclusion column (2.5 × 90 cm; GE Healthcare). Finally, fractions were loaded onto a Q sepharose Fast Flow column (GE Healthcare) equilibrated with buffer A, and bound protein was eluted with a linear gradient of NaCl (0.1–0.6 M in buffer A). Purified AcIB was dialyzed against Tris-HCl (25 mM, pH 7.5) with glycerol (20%) and stored at –20 °C. AcIB concentration was estimated as previously described with minor modifications.<sup>[54]</sup> The sample in Tris-HCl (100 mM, pH 8.5) and SDS (2%) was denatured by incubation for 15 min at 60 °C for, then further incubated with bathophenanthroline disulfonate (BPS, 0.2 mM) and dithionite (8 mM) for 30 min at 30 °C. The iron content of Fdx was determined by absorbance of the  $\text{Fe}^{2+}$ -BPS complex ( $\epsilon_{535} = 25\,100\text{ M}^{-1}\text{ cm}^{-1}$ ).

The gene encoding *aciC* from *Acinetobacter* sp. OC4 (accession: AB221118) was amplified by PCR with pTipQC2- $\text{Vdh}$ -AcIB-AciC as template DNA,<sup>[18]</sup> and inserted between NdeI and XhoI sites of a pET26a expression vector (culture and induction as for AcIB). The cells were harvested and resuspended in buffer B (sodium phosphate (50 mM, pH 8.0), NaCl (300 mM)) containing lysozyme (1 mg mL<sup>-1</sup>) and Benzonase (~50 U mL<sup>-1</sup>), and then disrupted by sonication. After centrifugation (39 191 g, 10 min, 4 °C), the supernatant was loaded onto a Ni-affinity column (Sigma-Aldrich) equilibrated with buffer B. The column was washed with buffer C (sodium phosphate (50 mM, pH 6.0), NaCl (300 mM), glycerol (10%)) and eluted with a linear gradient of imidazole (0–0.4 M in buffer C). The yellow-colored fractions were pooled and dialyzed against buffer D (Tris-HCl (25 mM, pH 7.5, glycerol (10%)). The dialyzed sample was loaded onto a DEAE Sepharose Fast Flow Column (GE Healthcare) equilibrated with buffer D, and bound protein was eluted with a linear gradient of NaCl (0–0.6 M in buffer D). After boiling and removal of denatured protein, the concentration of flavin was calculated ( $\epsilon_{473} = 9.2\text{ mM}^{-1}\text{ cm}^{-1}$ ).<sup>[55]</sup>

**In vitro reconstitution assay and kinetic analysis:**  $\text{VD}_3$  25-hydroxylase activity of  $\text{Vdh}_{\text{WT}}$  and its mutants was measured by reconstitution experiments. The reaction mixture (200  $\mu\text{L}$ ) for enzyme activity measurements comprised Tris-HCl (50 mM, pH 7.5), NaCl (100 mM), AcIB (10  $\mu\text{M}$ ) or spinach Fdx (100  $\mu\text{g mL}^{-1}$ ), AciC (1.0  $\mu\text{M}$ ) or spinach FdxR (0.1 U mL<sup>-1</sup>),  $\text{VD}_3$  (20  $\mu\text{M}$ ), NADH (200  $\mu\text{M}$ ; for AcIB-AciC system) or NADPH (200  $\mu\text{M}$ ; for spinach system), and PM $\beta$ CD (0.05%, w/v). The concentration of  $\text{Vdh}_{\text{WT}}$  (or mutant) was adjusted within the linear range of the assay. The reaction was initiated by addition of NADH/NADPH, and followed by incubation at 30 °C for 5 min. The reaction was stopped by addition of ethyl acetate (50  $\mu\text{L}$ ), and the mixture was extracted with ethyl acetate (800  $\mu\text{L}$ ). The product  $25(\text{OH})\text{VD}_3$  was detected by HPLC analysis as previously described.<sup>[18]</sup> The  $K_{\text{m}}$  and  $k_{\text{cat}}$  values for AcIB were estimated from Michaelis–Menten plots (triplicate experiments) with titration of AcIB (5–80  $\mu\text{M}$ ).

**Crystallization and X-ray structure determination:** Purified  $\text{Vdh}_{\text{T107A}}$  was concentrated to 20 mg mL<sup>-1</sup>, and  $\text{VD}_3$  was added (0.5 mM) for crystallization. All crystallization experiments were performed by the vapor-diffusion technique at 20 °C. An initial search for crystallization conditions was performed by using sparse matrix screen kits of Hampton Research (Aliso Viejo, CA) and Emerald Bio (Bedford, MA), and conditions were optimized by varying buffer pH and precipitant concentrations. Plate-shaped crystals (0.20 × 0.40 × 0.02 mm) grew in the solution containing Bis-Tris (0.1 M, pH 6.0–7.0), NaCl (0.2 M), and PEG 3350 (15–20%). X-ray diffraction



data were collected at beamline BL-5A of the Photon Factory (Tsukuba, Japan) with a Quantum 210r detector (ADSC Poway, CA). Prior to data collection, the crystal was soaked in cryoprotectant supplemented with glycerol (20%) and flash-cooled under a stream of nitrogen (100 K). The Vdh<sub>T107A</sub> crystal belongs to the space group C22<sub>2</sub>, with unit-cell dimensions  $a=61.4$ ,  $b=105.5$ ,  $c=142.0$  Å. The diffraction data were processed by using the program XDS.<sup>[56]</sup> The structure of Vdh<sub>T107</sub> was determined by the molecular replacement method by using the program MOLREP.<sup>[57]</sup> The X-ray model of Vdh-K1 (PDB ID: 3A50)<sup>[38]</sup> was used as a search model. The atomic coordinates and their  $B$ -factors were refined in REFMAC5,<sup>[58]</sup> and manual model corrections were performed with the graphic program COOT.<sup>[59]</sup> The stereochemical quality of the final refined model was checked by the program PROCHECK.<sup>[60]</sup> Crystallographic parameters and refinement statistics are summarized in Table 3. Molecular images were prepared with the program PyMOL (DeLano Scientific; <http://pymol.org/>). Electrostatic surface potentials were calculated by the Adaptive Poisson–Boltzmann Solver (APBS).<sup>[61]</sup>

**Biocatalytic production of 25(OH)VD<sub>3</sub> by nisin-treated *R. erythropolis* cells:** Expression vectors pTipQC2-Vdh<sub>WT</sub>-AcIB-AciC and pTipQC2-Vdh<sub>T107A</sub>-AcIB-AciC were constructed according to a previously described method.<sup>[18]</sup> The gene encoding BmGlcDH-IV was amplified by PCR with pET28a-BmGlcDH-IV as template DNA,<sup>[48]</sup> and was inserted between the NdeI and XhoI sites of the expression vector pNitQC2.<sup>[51]</sup> From this, a BmGlcDH-IV expression cassette (P<sub>nit</sub> promoter, BmGlcDH-IV sequence, and T<sub>thcA</sub> transcriptional terminator) was amplified by PCR, and inserted between the StuI and NsiI sites of the transposon-based expression vector to yield pTNR-KA-BmGlcDH-IV.<sup>[49]</sup> This was transformed into *R. erythropolis* JCM3201; the resulting strain was termed JCM3201-GlcDH. Expression of BmGlcDH-IV was confirmed by detecting GlcDH activity in the crude extract of the JCM3201-GlcDH, by monitoring NADH production (340 nm) in the presence of NAD<sup>+</sup> and D-glucose. JCM3201-GlcDH cells were transformed with pTipQC2-Vdh<sub>WT</sub>-AcIB-AciC or pTipQC2-Vdh<sub>T107A</sub>-AcIB-AciC, and grown in LB (20 mL) at 28 °C. Expression of Vdh<sub>WT</sub>/Vdh<sub>T107A</sub>, AcIB, and AciC was induced by addition of thiostrepton (0.5 µg mL<sup>-1</sup>) when cell growth reached the mid-log phase (OD<sub>600</sub> ≈ 0.7). At 24 h after induction, cells were harvested by centrifugation (1940g, 10 min, 4 °C), and the pellets were washed twice with potassium phosphate buffer (50 mM, pH 7.4), and resuspended (OD<sub>600</sub> = 5.0) in the same buffer (5 mL) supplemented with D-glucose (2%), glycerol (10%), VD<sub>3</sub> (2 mM), NADH (2 mM), PMβCD (1.5%), without or with nisin (0.5 mg mL<sup>-1</sup>). After incubation with shaking (120 rpm, 2 h), the reaction mixture (50 µL) was added to methanol (450 µL) and gently mixed. The resulting solution was centrifuged (20817g, 5 min, 20 °C), and the supernatant was analyzed by HPLC as previously described.<sup>[18]</sup> The repeated production (see text) was also performed with nisin-treated *R. erythropolis* JCM3201-GlcDH cells with pTipQC2-Vdh<sub>T107A</sub>-AcIB-AciC. The reaction buffer contained potassium phosphate (50 mM, pH 7.4), D-glucose (2%), glycerol (10%), VD<sub>3</sub> (2 mM), NADH (0.2 mM), PMβCD (1.5%), and nisin (0.5 mg mL<sup>-1</sup>). We found that the bioconversion rate was roughly constant for NADH ≥ 0.2 mM, and thus the concentration of NADH was reduced to 0.2 mM in this experiment (bioconversion mixture OD<sub>600</sub> = 10.0). The buffer was changed every 2 h, and four consecutive reactions (total, 8 h) were performed. The reaction product was analyzed by HPLC as previously described.<sup>[38]</sup>

**Accession number:** The atomic coordinates and structure details have been deposited in the Protein Data Bank, <http://www.pdb.org> under PDB ID 3VRM.

## Acknowledgements

The authors would like to thank Risa Yamagata for technical support. We also thank Dr. Akira Arisawa of MicroBiopharm Japan Co., Ltd. for the kind gift of the *aciB/aciC* genes. We are grateful to the beamline scientists at the Photon Factory (Tsukuba, Japan) for their kind assistance with X-ray diffraction experiments. This work was supported in part by the Development of Basic Technologies for Advanced Production Methods Using Microorganism Functions project of the New Energy and Industrial Technology Development Organization (NEDO) of Japan. This work was also supported in part by a Grant-in-Aid for Scientific Research from the Japan Society for the Promotion of Sciences (JSPS). Synchrotron radiation experiments were conducted under the approvals of 2011G129 at the Photon Factory.

**Keywords:** biosynthesis • crystal growth • cytochrome P450 • nisin • *Rhodococcus erythropolis* • vitamin D<sub>3</sub>

- [1] P. R. Ortiz de Montellano, *Chem. Rev.* **2010**, *110*, 932–948.
- [2] M. K. Julsing, S. Cornelissen, B. Bühler, A. Schmid, *Curr. Opin. Chem. Biol.* **2008**, *12*, 177–186.
- [3] F. Hannemann, A. Bichet, K. M. Ewen, R. Bernhardt, *Biochim. Biophys. Acta Gen. Subj.* **2007**, *1770*, 330–344.
- [4] A. Chefson, K. Auclair, *Mol. Biosyst.* **2006**, *2*, 462–469.
- [5] R. Bernhardt, *J. Biotechnol.* **2006**, *124*, 128–145.
- [6] V. B. Urlacher, M. Girhard, *Trends Biotechnol.* **2012**, *30*, 26–36.
- [7] C. J. C. Whitehouse, S. G. Bell, L.-L. Wong, *Chem. Soc. Rev.* **2012**, *41*, 1218–1260.
- [8] D. E. Prosser, G. Jones, *Trends Biochem. Sci.* **2004**, *29*, 664–673.
- [9] N. Sawada, T. Sakaki, M. Ohta, K. Inouye, *Biochem. Biophys. Res. Commun.* **2000**, *273*, 977–984.
- [10] N. Strushkevich, S. A. Usanov, A. N. Plotnikov, G. Jones, H.-W. Park, *J. Mol. Biol.* **2008**, *380*, 95–106.
- [11] K. Yamamoto, E. Uchida, N. Urushino, T. Sakaki, N. Kagawa, N. Sawada, M. Kamakura, S. Kato, K. Inouye, S. Yamada, *J. Biol. Chem.* **2005**, *280*, 30511–30516.
- [12] G. Jones, S. A. Strugnell, H. F. DeLuca, *Physiol. Rev.* **1998**, *78*, 1193–1231.
- [13] G.-D. Zhu, W. H. Okamura, *Chem. Rev.* **1995**, *95*, 1877–1952.
- [14] J. Sasaki, A. Miyazaki, M. Saito, T. Adachi, K. Mizoue, K. Hanada, S. Omura, *Appl. Microbiol. Biotechnol.* **1992**, *38*, 152–157.
- [15] K. Takeda, T. Asou, A. Matsuda, K. Kimura, K. Okamura, R. Okamoto, J. Sasaki, T. Adachi, S. Omura, *J. Ferment. Bioeng.* **1994**, *78*, 380–382.
- [16] Y. Fujii, H. Kabumoto, K. Nishimura, T. Fujii, S. Yanai, K. Takeda, N. Tamura, A. Arisawa, T. Tamura, *Biochem. Biophys. Res. Commun.* **2009**, *385*, 170–175.
- [17] J. Sikkema, J. A. M. de Bont, B. Poolman, *Microbiol. Rev.* **1995**, *59*, 201–222.
- [18] N. Imoto, T. Nishioka, T. Tamura, *Biochem. Biophys. Res. Commun.* **2011**, *405*, 393–398.
- [19] T. Fujii, Y. Fujii, K. Machida, A. Ochiai, M. Ito, *Biosci. Biotechnol. Biochem.* **2009**, *73*, 805–810.
- [20] K. Hayashi, K. Yasuda, H. Sugimoto, S. Ikushiro, M. Kamakura, A. Kittaka, R. L. Horst, T. C. Chen, M. Ohta, Y. Shiro, T. Sakaki, *FEBS J.* **2010**, *277*, 3999–4009.
- [21] K. Hayashi, H. Sugimoto, R. Shinkyo, M. Yamada, S. Ikeda, S. Ikushiro, M. Kamakura, Y. Shiro, T. Sakaki, *Biochemistry* **2008**, *47*, 11964–11972.
- [22] T. Sakaki, H. Sugimoto, K. Hayashi, K. Yasuda, E. Munetsuna, M. Kamakura, S. Ikushiro, Y. Shiro, *Biochim. Biophys. Acta Proteins Proteomics* **2011**, *1814*, 249–256.
- [23] A. Toyoda, H. Nagai, T. Yamada, Y. Moriguchi, J. Abe, T. Tsuchida, K. Nagasawa, *Tetrahedron* **2009**, *65*, 10002–10008.
- [24] T. Fujii, T. Narikawa, F. Sumisa, A. Arisawa, K. Takeda, J. Kato, *Biosci. Biotechnol. Biochem.* **2006**, *70*, 1379–1385.

- [25] S. G. Bell, F. Xu, E. O. D. Johnson, I. M. Forward, M. Bartlam, Z. Rao, L.-L. Wong, *J. Biol. Inorg. Chem.* **2010**, *15*, 315–328.
- [26] L. S. Koo, C. E. Immoos, M. S. Cohen, P. J. Farmer, P. R. Ortiz de Montellano, *J. Am. Chem. Soc.* **2002**, *124*, 5684–5691.
- [27] L. Ba, P. Li, H. Zhang, Y. Duan, Z. Lin, *Biotechnol. Bioeng.* **2013**; DOI: 10.1002/bit.24960.
- [28] S. G. Bell, J. H. C. McMillan, J. A. Yorke, E. Kavanagh, E. O. D. Johnson, L.-L. Wong, *Chem. Commun.* **2012**, *48*, 11692–11694.
- [29] T. L. Poulos, B. C. Finzel, A. J. Howard, *J. Mol. Biol.* **1987**, *195*, 687–700.
- [30] I. F. Sevioukova, C. Garcia, H. Li, B. Bhaskar, T. L. Poulos, *J. Mol. Biol.* **2003**, *333*, 377–392.
- [31] I. F. Sevioukova, H. Li, T. L. Poulos, *J. Mol. Biol.* **2004**, *336*, 889–902.
- [32] W. Zhang, S. S. Pochapsky, T. C. Pochapsky, N. U. Jain, *J. Mol. Biol.* **2008**, *384*, 349–363.
- [33] S. Tripathi, H. Li, T. L. Poulos, *Science* **2013**, *340*, 1227–1230.
- [34] M. Holden, M. Mayhew, D. Bunk, A. Roitberg, V. Vilker, *J. Biol. Chem.* **1997**, *272*, 21720–21725.
- [35] T. C. Pochapsky, T. A. Lyons, S. Kazanis, T. Arakaki, G. Ratnaswamy, *Biochimie* **1996**, *78*, 723–733.
- [36] A. Karyakin, D. Motiejunas, R. C. Wade, C. Jung, *Biochim. Biophys. Acta Gen. Subj.* **2007**, *1770*, 420–431.
- [37] J. D. Thompson, D. G. Higgins, T. J. Gibson, *Nucleic Acids Res.* **1994**, *22*, 4673–4680.
- [38] Y. Yasutake, Y. Fujii, T. Nishioka, W.-K. Cheon, A. Arisawa, T. Tamura, *J. Biol. Chem.* **2010**, *285*, 31193–31201.
- [39] D. H. Sherman, S. Li, L. V. Yermalitskaya, Y. Kim, J. A. Smith, M. R. Waterman, L. M. Podust, *J. Biol. Chem.* **2006**, *281*, 26289–26297.
- [40] Y.-T. Lee, R. F. Wilson, I. Rupniewski, D. B. Goodin, *Biochemistry* **2010**, *49*, 3412–3419.
- [41] C. Savino, L. C. Montemiglio, G. Sciara, A. E. Miele, S. G. Kendrew, P. Jemth, S. Gianni, B. Vallone, *J. Biol. Chem.* **2009**, *284*, 29170–29179.
- [42] W.-C. Huang, A. C. G. Westlake, J.-D. Marechal, M. G. Joyce, P. C. E. Moody, G. C. K. Roberts, *J. Mol. Biol.* **2007**, *373*, 633–651.
- [43] W. Yang, S. G. Bell, H. Wang, W. Zhou, N. Hoskins, A. Dale, M. Bartlam, L.-L. Wong, Z. Rao, *J. Biol. Chem.* **2010**, *285*, 27372–27384.
- [44] N. Urushino, K. Yamamoto, N. Kagawa, S. Ikushiro, M. Kamakura, S. Yamada, S. Kato, K. Inouye, T. Sakaki, *Biochemistry* **2006**, *45*, 4405–4412.
- [45] I. Wiedemann, R. Benz, H.-G. Sahl, *J. Bacteriol.* **2004**, *186*, 3259–3261.
- [46] H. E. Hasper, B. de Kruijff, E. Breukink, *Biochemistry* **2004**, *43*, 11567–11575.
- [47] T. Nagao, T. Mitamura, X. H. Wang, S. Negoro, T. Yomo, I. Urabe, H. Okada, *J. Bacteriol.* **1992**, *174*, 5013–5020.
- [48] T. Nishioka, Y. Yasutake, Y. Nishiya, T. Tamura, *FEBS J.* **2012**, *279*, 3264–3275.
- [49] K. I. Sallam, N. Tamura, T. Tamura, *Gene* **2007**, *386*, 173–182.
- [50] Z. Shao, W. A. Dick, R. M. Behki, *Lett. Appl. Microbiol.* **1995**, *21*, 261–266.
- [51] S. Nakashima, T. Tamura, *Appl. Environ. Microbiol.* **2004**, *70*, 5557–5568.
- [52] A. Hemsley, N. Arnheim, M. D. Toney, G. Cortopassi, D. J. Galas, *Nucleic Acids Res.* **1989**, *17*, 6545–6551.
- [53] T. Omura, R. Sato, *J. Biol. Chem.* **1964**, *239*, 2370–2378.
- [54] V. Tiranti, C. Viscomi, T. Hildebrandt, I. Di Meo, R. Mineri, C. Tiveron, M. D. Levitt, A. Prella, G. Fagioli, M. Rimoldi, M. Zeviani, *Nat. Med.* **2009**, *15*, 200–205.
- [55] A. Aliverti, B. Curti, M. A. Vanoni in *Methods in Molecular Biology, Vol. 131: Flavoprotein Protocols* (Eds.: S. K. Chapman, G. A. Reid), Humana, Totowa, **1999**, pp. 9–23.
- [56] W. Kabsch, *Acta Crystallogr. Sect. D Biol. Crystallogr.* **2010**, *66*, 125–132.
- [57] A. Vagin, A. Teplyakov, *J. Appl. Crystallogr.* **1997**, *30*, 1022–1025.
- [58] G. N. Murshudov, A. A. Vagin, E. J. Dodson, *Acta Crystallogr. Sect. D Biol. Crystallogr.* **1997**, *53*, 240–255.
- [59] P. Emsley, K. Cowtan, *Acta Crystallogr. Sect. D Biol. Crystallogr.* **2004**, *60*, 2126–2132.
- [60] R. A. Laskowski, M. W. MacArthur, D. S. Moss, J. M. Thornton, *J. Appl. Crystallogr.* **1993**, *26*, 283–291.
- [61] N. A. Baker, D. Sept, S. Joseph, M. J. Holst, J. A. McCammon, *Proc. Natl. Acad. Sci. USA* **2001**, *98*, 10037–10041.

Received: June 14, 2013

Published online on September 24, 2013